OVERVIEW ON THE INFLUENCE OF COANDĂ BLANKET CURVATURE ON COANDĂ DEVICE PERFORMANCE

Harijono Djojodihardjo
The Institute for the Advancement of Aerospace Science and Technology, Jakarta 15419, Indonesia

Keywords: *Circulation control, Coandă effect, Coandă MAV Flight Dynamics, Coandă MAV Fluid Dynamics, Micro air vehicle (MAV)*

Abstract

Capitalizing on the basic fundamental principles, the Fluid Dynamics and Flight Mechanics of a semi-spherical Coandă MAV configurations are revisited and analyzed as a baseline. To gain better understanding on the principle of Coandă MAV lift generation, a mathematical model for a spherical Coandă MAV is developed and analyzed from first physical principles. To gain further insight into the prevailing flow field around a Coandă MAV, as well as to verify the theoretical prediction presented in the work, a computational fluid dynamic CFD simulation for a Coandă MAV generic model are elaborated. Noting that extensive experimental investigations on jet deflection by curved walls showed that geometry greatly affects the Coandă effect flow, such as the curvature radius of a surface and jet thickness, parametric studies on the effect of varying exit jet heights and curvature of the Coandă device upper surface (Coandă blanket) on the Coandă effect is also presented.

1 Introduction

Since its founding [1, 2[, Coandă effect and Coandă jet have been found and utilized for flow control in many applications in engineering and health science, among others, such as in aircraft and vehicle technology [3-12], wind-turbines [13-14], and upper respiratory system [15-19]. Coandă MAV relates to the physical phenomenon whereby a stream of fluid at high velocity will attach to a curved surface rather than follow its original straight line direction. This stream of fluid will also entrain air from around it to increase the overall mass flow rate of the stream of air. Streamline curvature in the plane of the mean shear flow produces large changes in the turbulence structure of shear layers. These changes are usually an order of magnitude more important than normal pressure gradients and other explicit terms appearing in the mean-motion equations for curved flows [20]. In a seminal report on the effects of streamline curvature on turbulent flow, Bradshaw [20] categorized the tendency of a fluid jet placed near a surface to attach itself to the surface, and the attached jet growing more rapidly. He subdivided the Coandă effect into three distinct phenomenon, which are illustrated in Figure 1. The effect whereby a jet attached to a convex surface grows more rapidly than the wall jet on a plane surface, according to [20, 21], should be more appropriately referred to as 'Coandă effect'.

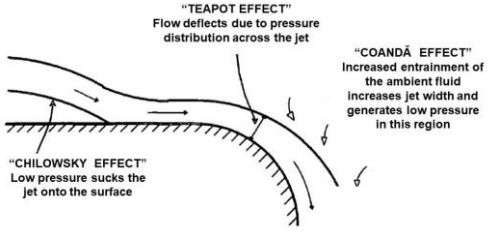

Figure 1 Coandă Flow Characteristic (adapted from [21])

Dumitrache etal [22] have shown that a the steady two-dimensional, laminar and turbulent flow of an incompressible fluid that develops a jet-sheet on a cylinder surface, i.e., a Coandă flow, can be well approximated by similar solutions for both the laminar and the turbulent regime.

Capitalizing on the basic fundamental principles, the Fluid Dynamics and Flight Mechanics of a semi-spherical Coandă MAV configurations are revisited and analyzed as a baseline. The dependence of the performance of Coandă MAV or device, or more generally of Coandă effect, on various geometric factors will be of great interest. Therefore, in depth understanding of such influence on this phenomenon will be relevant in producing optimum design performance of Coandă MAV or device.

For a Coandă MAV, lift is produced in two ways. Firstly, due to the change of direction of the airflow downwards, and secondly, due to the entrainment of air from above which causes a region of low pressure above the body.

To gain better understanding on the principle of Coandă MAV lift generation, a mathematical model for a spherical Coandă MAV is developed and analyzed from first physical principles. To gain further insight into the prevailing flow field around a Coandă MAV, as well as to verify the theoretical prediction presented in the work, a computational fluid dynamic CFD simulation using commercial software for a Coandă MAV generic model are reviewed and elaborated. Particular attention is given to the hovering state. The mathematical model based on first principle and corresponding derived performance measures capability in describing the physical phenomena of the flow field of the semi-spherical Coandă MAV will first be assessed. The relationships between the relevant parameters of the mathematical model of the Coandă MAV to the forces acting on it are elaborated subsequently.

Noting that extensive experimental investigations on jet deflection by curved walls showed that geometry greatly affects the Coandă effect flow, such as the curvature radius of a surface and jet thickness, parametric studies on the effect of varying exit jet heights and curvature of the Coandă device upper surface (Coandă blanket) on the Coandă effect will be reviewed and assessed.

2 Brief Review of Coandă effect

Some experimental results related to the Coandă effect have been presented by Crifoi and Doroftei [23], based on their experiments on a laboratory testing device. Some advantages and disadvantages to applying Coandă effect to a flying vehicle found are reducing the pressure near the of the convex surface, protected screw, vertical takeoff and landing. This technical solution can bring some benefits through a suited sizing and geometry with vehicle mass. Figure1 depicts typical fluid jet initially flowing tangentially over a convex wall (adapted from [22] and [23])

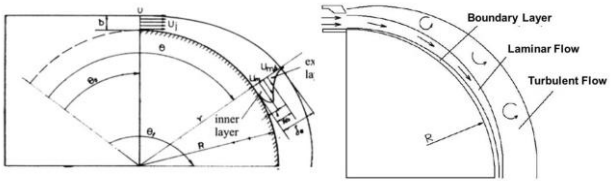

Figure 2. Fluid jet in near convex wall (adapted from [22] and [23])

In an earlier work, investigation has been carried out on the mathematical model of Coandă MAV by Djojodihardjo and Ahmed [7] and Ahmed et al [8-10], which was based on first principles and is used as a baseline reference for successive development. For Coandă MAV with the configuration depicted in Figure 3(a), an actuator rotor can be visualized to be located at the center of the body. For conceptual development, the dimension of the rotor can be set to be small as necessary. Part of the flow being drawn by the actuator can be utilized for lift (like in a helicopter), and part of it will be utilized for introducing radial flow on the surface of the body as a Coandă jet blanket. Momentum analysis is carried out in the analysis of Coandă effect related to finding the relevant aerodynamic forces and defining the Coandă MAV performance parameters. The latter is developed for a baseline and simplified semi-spherical Coandă MAV as depicted in Figure 3(a) [7-9].

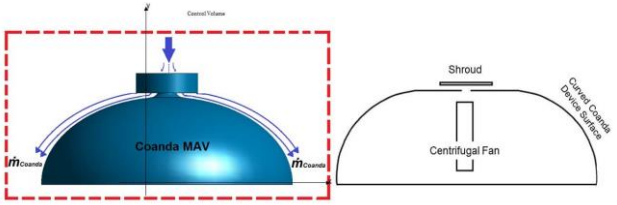

(a) (b)

Figure 3: Two examples of possible configurations of semi-spherical Coandă MAV to produce Coandă jet over its upper surface; (a) from [7-9]; (b) from [24]

Focusing on the evaluation of the development of jet flow along the Coandă curvature, as well as the performance of the Coandă effect caused by geometrical variations in exit jet height and Coandă curvature angle via the 2D computational fluid dynamics (CFD) approach, Gan et al [24] considered an MAV device as exhibited in Figure 3(b).

Earlier work [7-10] gave a comparison of analytical and CFD models for the Performance Measure P_{M2} defined by Total Lift L_{MAV}/ Inlet Velocity $V_{j\text{-}in}$ for semi-spherical Coandă as depicted in Figure 3(a). Results reported there clearly exhibits the noticeable influence of the ratio of the jet slot thickness h to the reference radius R_o, as exhibited in Figure 5. The influence of the jet inlet velocity on lift enables designers to appropriately select the right propulsion system specifications for the Coandă MAV.

The resulting Lift as a function of input jet velocity diagram for each of these configurations has also been obtained. CFD simulations were carried out, which were performed using steady RANS, employing two equations k-ω Shear Stress Transport (SST) turbulence model. In the solution procedure followed, simple pressure-velocity coupling scheme with the least squares cell base as discretization gradient has been applied; second order upwind for the momentum equation and the turbulent kinetic energy were also imposed.

These CFD simulations have been carried to investigate the influence of the jet inlet radius on the air vehicle performance (lift), The CFD simulations were carried out for two inlet jet radius, R_i=5 mm and Ri=50mm for the baseline semi-spherical Coandă MAV configurations studied.

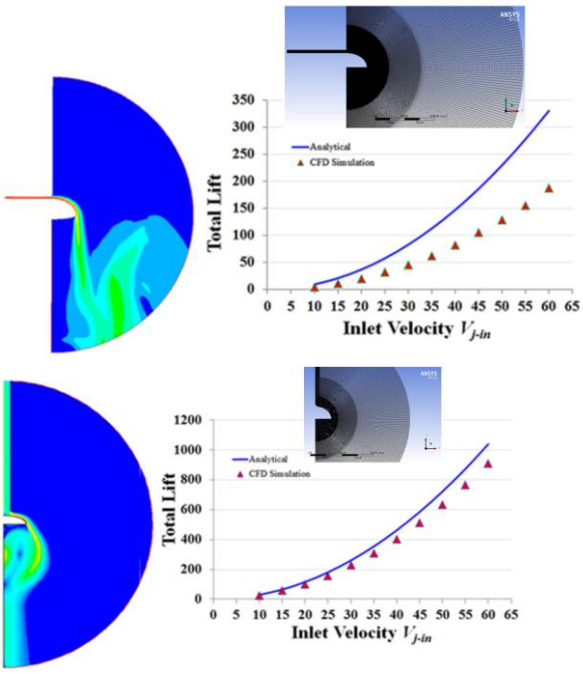

Figure 5 Lift versus input jet velocity for different Coandă jet inlet configurations.

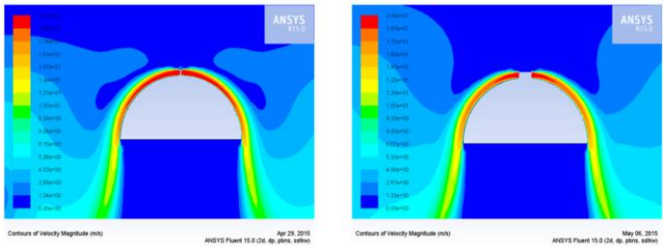

(a) (b)

Figure 6 CFD simulation on two Coandă MAV configurations: a) Ri=5 mm, b) R_i=50mm. Relatively symmetrical Coandă effect velocity magnitude contours are exhibited.

Some physically significant results are exhibited in Figures 5, 6 and 7, which show the velocity field in the Coandă jet and its surrounding due to symmetrical Coandă effect.

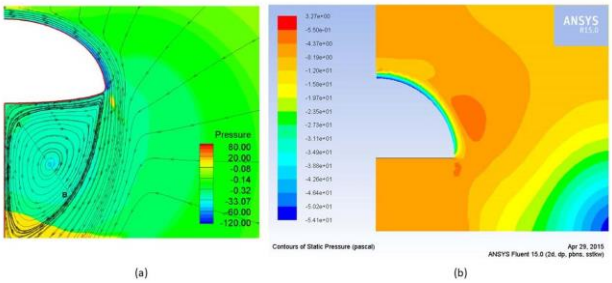

(a) (b)

Figure 7. CFD simulation results plot of flow field pressure contours for the semi-spherical Coandă MAV;(a) Mirkov and Rasuo [25]; (b) and CFD simulation results from [7-9]

The results are presented as velocity magnitude contours, which exhibit the influence of the inlet radius on the flow field around the Coandă blanket.

The related work carried out in [24] utilized a logarithmic spiral surface, and the development of jet flow along the Coandă curvature was investigated. Cutbill [21] mentioned that for a logarithmic spiral, the local radius of curvature is proportional to distance from the flow origin, an arrangement that leads to the development of a self-preserving wall jet growing linearly with downstream distance. The rate of growth of these equilibrium layers is highly sensitive to the ratio of shear-layer thickness to radius of curvature. Two-dimensional computational fluid dynamics numerical simulations were carried out to measure the velocity profile, jet width growth, maximum velocity decay, and surface static pressure along the curvature surface. For this work, contour plots of velocity magnitude and velocity profiles across the jet at different measuring stations along the Coandă surface are shown in Figures 8.

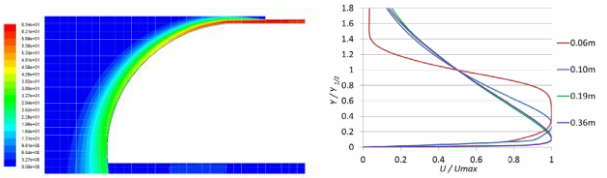

Figure 8: (a)Contour plot of velocity magnitude (m/s); (b) Velocity profiles across jet at different measuring stations along the Coandă surface.

Note also that following Launder and Rodi [26], for a logarithmic spiral, the local radius of curvature is proportional to distance from the flow origin, an arrangement that leads to the development of a self-preserving wall jet growing linearly with downstream distance. The Coandă effect has been introduced into lift generation designs. 2D computational fluid dynamics numerical simulation is adopted to measure velocity profile, jet width growth, maximum velocity decay, and surface static pressure along the curvature surface. Results of a parametric study on the effect of varying exit jet heights on the Coandă effect show that jet width grows proportionally along the curved surface, and the proportional decay of maximum velocity and surface pressure is lower than the atmospheric pressure. A wider exit jet height produces lower static pressure on the unmanned aerial vehicle surface and a slower maximum velocity decay. Overall parametric analysis of varying exit jet heights can show the effective range of d/R for a particular Coandă effect based MAV configuratoion. Other geometrical design effect on the performance of Coandă effect based MAV or device will be essential on their conception, design and operation. Associated with it, one could refer to Newman's study [27] which identified two associated effects of the phenomenon: pressure on the deflection surface is lower than that of the surroundings, and the surrounding fluid entrained into the jet increases.

3 Mathematical Models for Semi-Spherical (Saucer-like) Coandă MAV Configurations

Based on first principles, and utilizing the conservation equations, mathematical model developed as indicated in [7-9], and will be discussed and assessed in view of related CFD simulation with reference to various aspects. Specific performance measures can be derived, which to some extent can describe the physical phenomena of the flow field of Coandă MAV. The relationships between the relevant parameters of the mathematical model of the Coandă MAV to the lift are summarized subsequently.

Various configurations for Coandă MAV have been studied. In the configuration depicted in Figures 3 (a) [7-9], an actuator rotor located at the center of the body has been utilized. For conceptual development, the dimension of the rotor can be set to be small. Although part of the flow being drawn by the actuator can be utilized for lift (like in a helicopter), the present focus is the radial flow part for Coandă jet blanket on the surface of the body.

Two-dimensional momentum analyses are carried out in order to identify the performance parameters. The performance parameters are related to the two effects; these are the Coandă jet effect and the actuator disc effect.

The contribution of Coandă effect to the generation of lift capability of Coandă MAV is

rigorously analyzed. First the analysis will address the Coandă effect for lift by applying the fundamental conservation analysis on the control volume (CV) (red dashed rectangle in Figure 9).

The continuity equation, which reduces to that alongside the Coandă Blanket gives

$$V_{j\text{-}out} = \frac{\dot{m}}{2\pi\rho R_i h_i} = \frac{R_i h_i}{R_o h_o} V_{j\text{-}in}$$
$$V_{j\text{-}R} = \frac{\dot{m}}{2\pi\rho R_i h_i} = \frac{R_i h_i}{R h_R} V_{j\text{-}in} \quad (1)$$

The Momentum equation in the *y*-(vertical) direction can be differentiated into the contribution due to the Coandă Blanket momentum and the pressure difference on the body due to Coandă Blanket:

$$\begin{pmatrix}\text{Total Lift force due to Coandă Blanket}\end{pmatrix} = \begin{pmatrix}\text{Vertical component of momentum balance due to Coandă Blanket}\end{pmatrix} + \begin{pmatrix}\text{Pressure difference on the body of MAVsubject to Coandă Blanket}\end{pmatrix} \quad (2)$$

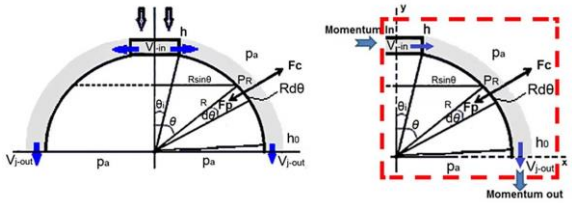

Figure 9: Schematic of Coandă jet (Blanket) for a Semi-Spherical MAV

The lift contribution from the momentum flux through the control volume CV in the vertical direction is given by:

Force in the y-direction = Momentum out in the y-direction - Momentum out in the y-direction (3)

Since, in the radial direction, the Momentum In does not contribute to lift, and then the momentum equation in the y-direction for the CV depicted in Figure 9 is:

$$F_{CoJB} = \dot{m} V_{j\text{-}out} = 2\pi R_i h_i \rho \cdot V_{j\text{-}in} \cdot V_{j\text{-}out} \quad (4)$$

The contribution of lift from the pressure difference between the upper (curved MAV body covered by Coandă Blanket) and the lower part of the MAV body, is given by:

$$F_{IPD} = \pi\left(R_o^2 - R_i^2\right) p_a - \int_{\theta_i}^{\theta_0} \left(p_a - \frac{h}{R}\rho\left(\frac{\dot{m}}{2\pi\rho R h}\right)^2_{j-R}\right) 2\pi R^2 \sin 2\theta d\theta \quad (5)$$

The jet flow assumed uniform outflow separating at the sharp edge of the Coandă MAV curved surface. Then the contribution of the pressure difference across the surfaces of the MAV body for lift for the significant value of θ_i, is given by

$$F_{IPD} = \left(\frac{\dot{m}^2}{4\pi\rho h R}\right)_{j-R} \quad (6)$$

Hence the total lift due to Coandă jet blanket momentum and Coandă jet blanket induced pressure difference is given as

$$Lift_{\substack{Spherical-\\ Coanda\ jet\ Blanket+\\ induced\ pressure\ difference}} = 2\pi R_i h_i \rho V_{j\text{-}in} \times V_{j\text{-}out} + \left(\frac{\dot{m}^2}{4\pi\rho R h}\right)_{j-R} = \dot{m} \times V_{j\text{-}out} + \frac{1}{2}\dot{m} V_{j\text{-}R} \quad (7)$$

Therefore, the Coandă MAV has additional lift given in (6), due to the presence of the Coandă blanket, in comparison to a simple micro air vehicle powered by actuator disk only. It should be noted that a more exact approach requires additional information, i.e. the energy conservation equation, which is then utilized as the fourth equation. This is elaborated subsequently.

Applying the energy conservation equation on the same control volume, which has been redrawn for convenience in Figure 10, assuming uniform properties across the sectional areas at the input and output of the Coandă jet blanket and ignoring the entrainment energy exchange between the ambient air and the Coandă jet blanket, the energy equation can be written as:

$$\left(\frac{p}{\rho}\right)_{in} + \frac{1}{2}\left(V_{j\text{-}in}^2\right) = \left(\frac{p}{\rho}\right)_{out} + \frac{1}{2}\left(V_{j\text{-}out}^2\right) \quad (8)$$

which is essentially the Bernoulli equation along any streamline between the inlet and the outlet sections. The contribution of the entrainment energy exchange along the Coandă jet blanket can later be incorporated, such as by adopting certain assumptions as a heuristic approach or, applying the complete viscous equation by numerical simulation or CFD approach. The latter should be carried out for more meticulous approach, using the present simplified analytical approach as guidelines.

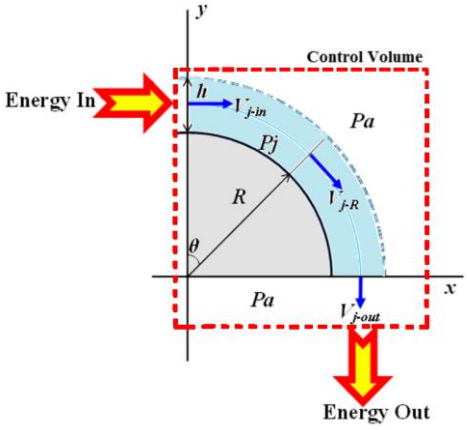

Figure 10 Schematic of the control volume around the MAV for the application of the energy conservation equation (not into scale)

At the same time, the CFD results, by appropriate considerations of the relevant parameters utilized there can be used in developing the heuristic approach as well as for validating and assessing the merit of the analytical approach. Noting that from the outset, the flow is considered incompressible, equation (7) reduces to,

$$\frac{1}{2}\rho V_{j\text{-}in}^{2} = \frac{1}{2}\rho V_{j\text{-}out}^{2} \qquad (9)$$

Hence, by the application of the conservation energy principle for incompressible flow, and assuming ambient pressure at the inlet and outlet of the Coandă jet blanket and neglecting the energy exchange between the ambient air and the Coandă jet blanket, the following velocity relationship between the inlet and outlet sections of the Coandă jet blanket is given by

$$V_{j\text{-}out} = V_{j\text{-}in} \qquad (10)$$

This latter equation should simplify the solution given in equation (7) and reduce the use of idealization or the number of assumption since fewer unknowns are included in the equations. Combining equations (7) and (10) yields:

$$Lift_{\substack{Spherical\text{-}\\CoJB+IPD}} = \frac{3}{2}\dot{m}V_{j-in} \qquad (11)$$

The results will be assessed posteriori by using more structured CFD simulations, which incorporate the effect of viscosity through the use of Navier-Stokes equation, although the latter also contain uncertainties and inaccuracies.

4 Results and Discussions

To assess the merit and plausibility of the theoretical analysis using first principles carried out here, a comparison of the theoretical prediction for the performance measures *PM*1, *PM*2 and *PM*3 given by equation (26 - 28) are compared with CFD simulation carried out using ANSYS Fluent® for Spherically Shaped Coandă MAV. The results are depicted in figures 12 and 13. The simulation was performed using steady RANS with two equations k-ω Shear Stress Transport (SST) turbulence model has been used in [29]. Simple pressure-velocity coupling scheme with the least squares cell base as discretization gradient was applied in the solution method together with second order upwind for the momentum equation and the turbulent kinetic energy.

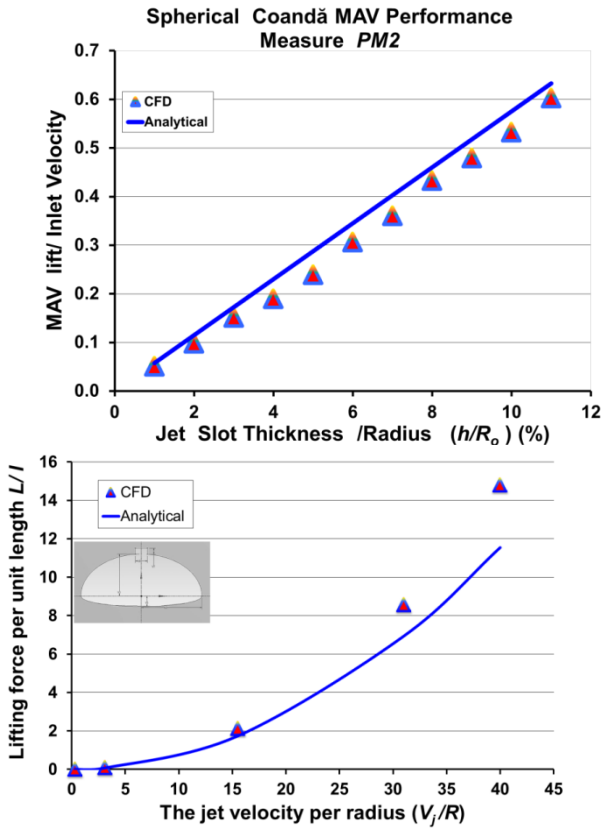

Fig. 12 Performance measure for spherical Coandă MAV for a) various jet slot thickness at different jet velocity and b) various jet inlet velocity at constant jet thickness (*h*=50mm).

For the performance *PM*2 as depicted in Fig. 12a, the influence of the ratio of the jet slot thickness h to the reference radius R_o which influence the jet inlet velocity is clearly

noticeable. In addition to the above performance measures, the influence of the jet inlet velocity on the air vehicle performance "lift" may also be of interest from designer's point of view, which enables them to befittingly select the right propulsion system for such MAV. The jet inlet velocity influence on performance of Spherical Coandă MAV at constant jet thickness (h = 50 mm) is depicted in Fig. 12b.

For Cylindrical Coandă MAV the corresponding theoretical prediction for PM2 is

$$PM2_{\substack{Cylinderical-\\CoMAV}} = \frac{Lift_{CoJB+IPD}}{Coandă\ jet\ inlet\ Velocity} = \frac{\rho V_{j-in}^2 l\left(\frac{h^2}{t}\right)+\frac{1}{2}\rho\left(\frac{h}{t}V_{j-in}\right)^2 Rl}{V_{j\text{-}in}} \quad (12)$$

For comparative and validation purposes, Fig. 13 (a) and (b) are produced to assess the present theoretical prediction with CFD simulation results for the case deliberated by Schroijen and van Tooren [28] for cylindrical Coandă MAV, for h/R= 0.075 at two different jet inlet velocities.

Relatively good qualitative agreements between the theoretical results and CFD simulations shown there lend support to the present analysis, noting that in the analytical study carried out here many simplification have been introduced, while in the CFD simulation, the full Navier-Stokes equation for incompressible fluid was used.

Fig. 14 exemplifies the effect of viscosity that can be revealed by CFD simulation for two different locations of the Coandă jet introduction. The CFD images exhibited in Fig. 14 (a) and (b) show the velocity magnitude contours for the given configuration and inlet conditions for cases considered by Mirkov and Rasuo [25] and Ghozali [29].

Figure 15 shows structured numerical mesh used in the flow domain. Through meticulous attempts and grid sensitivity studies the size of the mesh cells was generated small to enable visualizations of the flow around the whole body with best details.

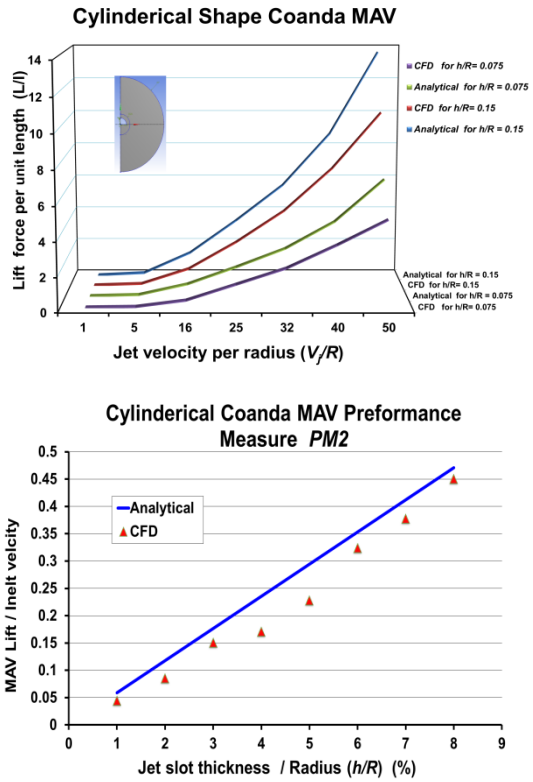

Fig.13 Performance measure comparison between mathematical and CFD models for Cylindrical Coandă MAV for various (a) Inlet velocity and (b) Jet slot thickness.

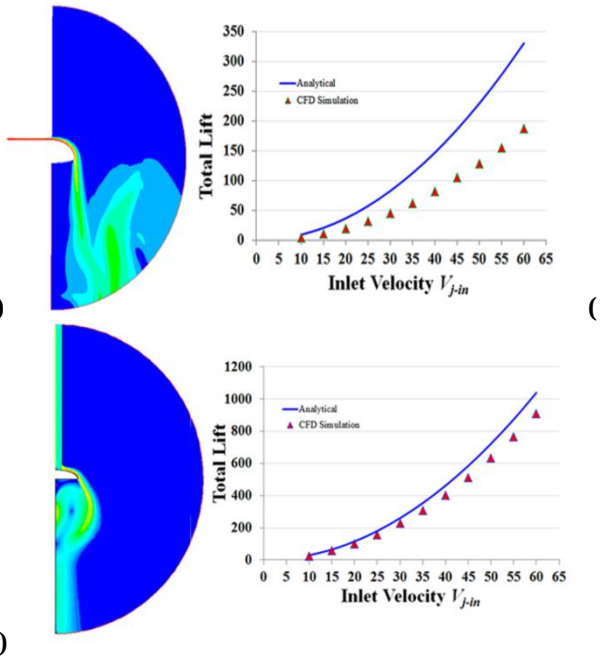

(a) **(**

b)

Fig. 14 Lift versus input jet velocity for similar configuration considered in (a) Mirkov and Rasuo [16], (b) Ghozali [27].

The numerical study was performed with a moderately small Reynolds number, Re = 68458, based on mean velocity and jet inlet height. The velocity is uniform ($V_{j\text{-}in}$ = 20 m/s) across the inlet which has a thickness of 0.05 m. The number of the mesh cells was 52830, and the mesh quality was found to be acceptable. The orthogonality quality was 4.96943e-01, which should be acceptable from the ANSYS orthogonality quality requirements. As elaborated by Djojodihardjo and Ahmed [7] and Ahmed et al., [8, 9] computation mesh for these CFD calculation has been deemed to be acceptable.

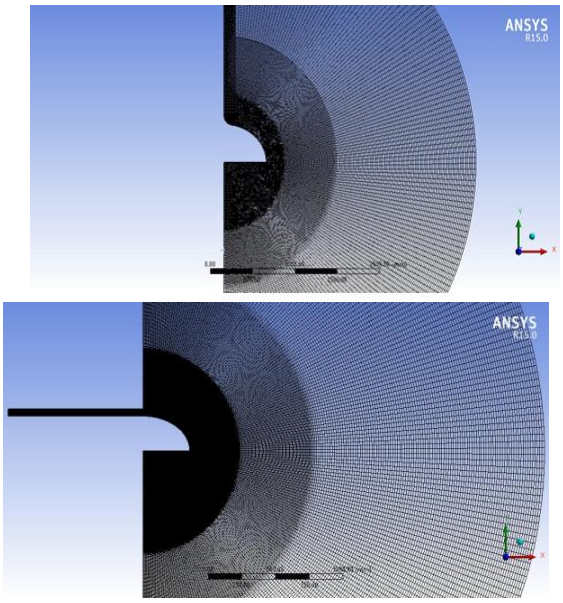

Fig.15 Mesh details for similar configuration considered in (a) Mirkov and Rasuo [25], (b) Ghozali [29]

The influence of the inlet jet radius on the air vehicle performance (lift) is also investigated using the CFD simulation. The results are presented as velocity magnitude contours, which were carried out for two inlet jet radius, R_i = 5 mm and R_i = 50 mm and as shown in Figure 16.

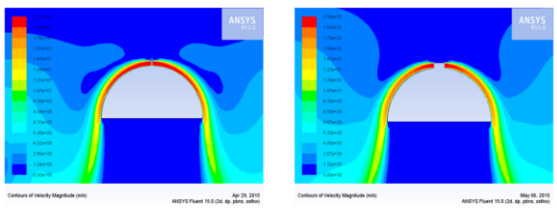

Fig. 16 Symmetrical Coandă effect-velocity magnitude contour with different inlet radius (a) R_i = 5 mm, (b) R_i = 50 mm.

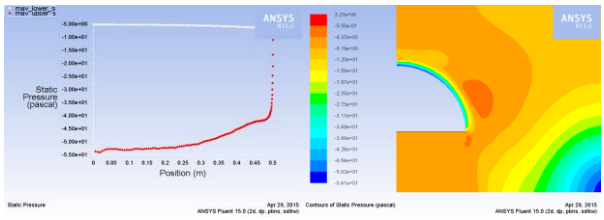

Fig.17 Comparison between the CFD simulation and plot for pressure contours along semi-spherical Coandă MAV surface.

For the semi-spherical Coandă jet MAV, the CFD simulation and visualization results are exhibited in Figure 17, which exhibit the pressure contours along semi-spherical Coandă MAV surface obtained by CFD simulation results (left), and the associated static pressure color-coded contour (right).

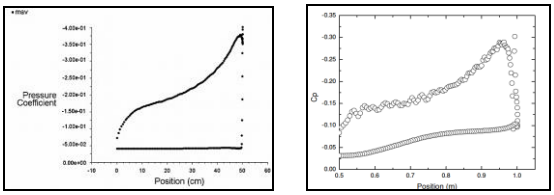

Fig. 18 Comparison of the coefficient of pressure on the Coandă blanket surface; (a) CFD Simulation in [7-9], (b) simulation by Mirkov and Rasuo [25].

The numerical study was performed with a moderately small Reynolds number, *Re* = 68458, based on mean velocity and jet inlet height. The velocity across the inlet, which has a thickness of 0.05 m, is uniform ($V_{j\text{-}in}$ = 20 m/s). The number of the mesh cells was 52830, and the mesh quality was found to be acceptable. The orthogonality quality was 4.96943e-01, which is acceptable from the ANSYS orthogonality quality requirements. Figure 18 compares the coefficient of pressure on the Coandă blanket surface; (a) CFD Simulation by Djojodihardjo and Ahmed [7] and Ahmed et al. [8, 9], (b) simulation by Mirkov and Rasuo [25].

For comparative purposes, the performance of the Coandă effect due to the variations in exit jet height obtained by Gan et al [24] is

illustrated in Figure 19 as Contour plot of velocity magnitude (m/s) velocity profiles across jet at different measuring stations along the Coandă surface (b). Measuring stations along the Coandă curvature are placed at 10 deg intervals from 0 deg to 90 deg.

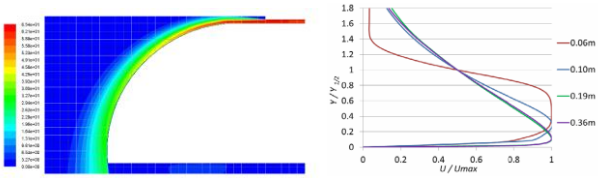

Figure 19. (a) Contour plot of velocity magnitude (m/s). (b) Velocity profiles across jet at different measuring stations along the Coandă surface.

The velocity profiles have been non-dimensionalized by the local maximum velocity U_{max} and half width $Y½$. Half width $Y½$ is defined as the y value when the velocity is

$$U = U_{max} / 2 \qquad (13)$$

Measuring the station at 0.1 m is the start of the logarithmic spiral surface, while measuring at 0.36 m is the end point of the UAV body.

8 Conclusions

Based on these preliminary results, further work will be carried out in the paper for CFD simulation and associated parametric study to elaborate and provide detailed information on the flow situation schematically modeled in Figure 20, which depicts estimated flow structure in and around the Coandă blanket for the Coandă device, which has been synthesized using information obtained in the references [1-9].

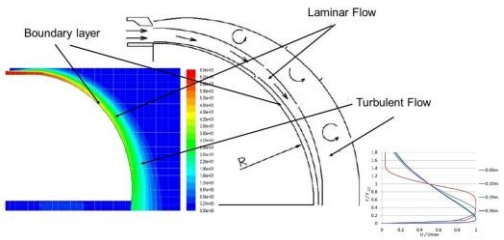

Figure 7. COANDĂ Jet over curved surface and preliminary estimated flow structure

The review of the parametric study carried out shows that the Coandă effect achieves stable performance after certain geometric variations, which can lead to the conclusion that an optimal design solution for a Coandă UAV exists. These initial numerical results can be used for further experimental investigations to develop a flying prototype that is based purely on the Coandă effect.

References

[1] Coandă, H. "Perfectionnement aux propulseurs," Brevet d'invention France, no. 796.843 /15.01.1935.
[2] Coandă, H. and C. France, "Device for deflecting a stream of elastic fluid projected into an elastic fluid," US Patent Office, 2,052,869. 1936.
[3] Gad-el-Hak, M. Introduction to flow control - in flow Control. Fundamentals and Practices, Springer-Verlag,
1998, pp. 1-108.
[4] Gad-el-Hak, M. Flow Control - Passive, Active and Reactive Flow Management, Cambridge University Press,
London, United Kingdom, 2000.
[5] Jones, G.S., Viken, S.A., Washburn, A.E., Jenkins, L.N., Cagle, C.M., An active flow circulation controlled flap
concept for general aviation aircraft applications, Flow Physics & Control Branch NASA Langley Research
Center, AIAA-2002-3157.
[6] Englar, R.J., Smith, M.J., Kelley, S.M, Rover, R.C., Application of circulation control to advanced subsonic transport aircraft, Part I: Airfoil development, Journal of Aircraft. 31(5) (1994) 1160-1168.
[7] Djojodihardjo, H and Ahmed, RI, Analytical, Computational Fluid Dynamics and Flight Dynamics of Coandă MAV, IOP Conf. Series: Materials Science and Engineering 157 (2016) 012002
[8] Ahmed, RI, Abu Talib, AR, Mohd Rafie, AS, Djojodihardjo, H, Aerodynamics and flight mechanics of MAV based on Coandă effect, Aerospace Science and Technology, 2017, V62, pp 136-147
[9] Ahmed, RI, Djojodihardjo, H, Abu Talib, AR, First principle analysis of Coandă Micro Air Vehicle aerodynamic forces for preliminary sizing, Aircraft Engineering and Aerospace Technology, Volume89, Issue 2, pp 231-245, 2017
[10] Ahmed, RI, Djojodihardjo, H, Abu Talib, AR, Mohd Rafie, AS, Review on Progress and Application of Active Flow Control Devices - Coandă Effect on Unmanned Aerial Vehicles, Pertanika Journal of Scholarly Research Reviews- PJSRR (2017) 3(1): 113-137
[11] Jones, G. S. and Englar, R.J., "Advances in pneumatic-controlled high-lift systems through pulsed blowing",AIAA-2005-3411.

[12] Kweder, J., Panther, C.C., Smith, J.E., Applications of circulation control, yesterday and today, International
Journal of Engineering, 195; 4(5) (2011) 411-429.
[13] Englar, R.J., Experimental Investigation of The High Velocity Coandă Wall Jet Applied to Bluff Trailing Edge Circulation Control Airfoils, David W. Taylor Naval Ship Research And Development Center Report 4708, September 1978
[14] Djojodihardjo, H., Abdul Hamid, M. F. Jaafar, A. A., Basri, S., Romli, F. I., Mustapha, F., Mohd Rafie, A. S. and Abdul Majid, D. L. A., Computational Study on the Aerodynamic Performance of Wind Turbine Airfoil Fitted with Coandă Jet, Hindawi Publishing Corporation Journal of Renewable Energy, Vol 2013, Article ID 839319, 17 pages
[15] Schoenherr, A., Bailly, L., Boiron, O., Lagier, A., Legou, T., Pichelin, M., Caillibotte, G. and Giovanni, A., Realistic glottal motion and airflow rate during human breathing. *Medical Engineering and Physics* 1 (2015).
[16] Schoenherr, A., Glottal motion and its impact on airflow and aerosol depositionin upper airways during human breathing. PhD Thesis, Institut de Recherchesur les Phénomènes Hors Équilibre, Ecole Centrale du Marseille (2015).
[17] Erath B. and Plesniak, M. W., The occurrence of the Coandă effect in pulsatile flow through static models of the human vocal folds. *J. Acoust. Soc. Am.* 120 (2006).
[18] Mittal, R. B., Erath, D. and Plesniak, M. W., Fluid dynamics of human phonation and speech, *Annual Review of Fluid Mechanics* (2013)
[19] Djojodihardjo, H and Ahmed, RI, CFD Simulation of Coandă Effect on the Upper Respiratory System, Journal of Medical Imaging and Health Informatics, Vol. 6, 1–9, 2015
[20] Bradshaw, P., *Effects of streamline curvature on turbulent flow*, Advisory Group for Aerospace Research and Development, Paris, France (1973).
[21] Cutbill, S., A study of the turbulent flow of a high speed Coandă jet, PhD Thesis, U Durham, 1998
[22] Dumitrache, A, Frunzulica F and Ionescu, T.C., Mathematical Modelling and Numerical Investigations on the COANDĂ Effect, INTECH 2012
[23] Crivoi, O and Doroftei, I., 2016 *IOP Conf. Ser.: Mater. Sci. Eng.* **147** 012082, 2016
[24] Gan, C-Y, Sahari, K.S.M. and Tan, C.S., Numerical investigation on Coandă flow over a logarithmic surface, JMechSci&Tech, 2015, V29,7, pp 2863–2869
[25] Mirkov, N and Rasuo, B., Numerical Simulation of Air Jet Attachment to Convex Walls and Applications, ICAS 2010-621
[26] Launder, B.E. and Rodi, W., The Turbulent Wall Jet Measurements and Modeling, AnnRevFlMech 1983
[27] Newman, B. G., The deflexion of plane jets by adjacent boundaries- Coandă effect, Boundary Layer and Flow Control, 1 (1961) 232-264.
[28] Schroijen, M., Van Tooren, M., MAV propulsion system using the Coandă effect, American Institute of Aeronautics and Astronautics. AIAA/ASAME/SAE/ASEE. Exhibit. USA: Denver Colorado, Joint Propulsion Conference, (2009) 1-10.
[29] Ghozali, Analysis of Coandă Effect Using Computational-Fluid-Dynamic", Thesis, Universitas Gajah Mada, Indonesia, 2013.

Contact Author Email Address

mailto:harijono@djojodihardjo.com

Copyright Statement